Approximating Aerodynamic Response of the Space Elevator to Lower Atmospheric Wind

David D. Lang[1]

[1]*David D. Lang Associates, Seattle WA.*

Abstract: This presents findings of time-domain simulation studies of the space elevator using the Generalized Tethered Object Simulation System (GTOSS). Brief overviews of the mathematical models comprising GTOSS are presented. A simplified, subsonic, flat-plate aerodynamic model is employed to simulate air loads. The physical configuration of the elevator as it manifests itself within GTOSS is described. In an attempt to discover the nature of possible wind-induced failure modes, the elevator's response, both with and without a climber on the ribbon, is determined for variations in wind speed and ribbon width.

1. Introduction

Since the space elevator is at the preliminary stage of undergoing design feasibility analysis, this paper explores the dynamic response of some elevator configurations to certain extreme atmospheric conditions to determine the degree to which wind loading may threaten the elevator. This paper attempts to answer such questions as:

(a) what might be the elevator's failure modes due to winds, (b) what level of wind is sufficient to destroy the elevator, (c) how might the presence of a climber in the lower atmosphere effect the response of the elevator to wind, (d) how might the presence of a climber parked at LEO altitude effect the response of the elevator to wind?

2. GTOSS Overview

The **G**eneralized **T**ethered **O**bject **S**imulation **S**ystem is a time-domain dynamics simulation code, developed by the author in 1982 to provide NASA with the capability to simulate the dynamics of combinations of space objects and tethers to accomplish flight safety certification for the Shuttle Tethered Satellite System (TSS) missions. Since then, GTOSS has undergone continuous evolution and validation, being applied at some stage in the formulation of virtually every US tethered space experiment flown to date; more than 25 aerospace organizations have employed it. The design criteria for GTOSS featured generality, thus allowing its current use in simulating space elevator behavior. Below is an overview of its features.

• Multiple rigid bodies, with 3 or 6 degree of freedom, connected in arbitrary fashion by multiple tethers, all subject to natural planetary environments, including sophisticated models for earth attributes as well as more rudimentary models for the other planets.

• Tethers represented by either *massless* or *massive* models. The *massive* (called *finite*) tether model is a "point synthesis" approach employing a constant number of up to 500 nodes, specifiable by tether (500 being a system configurable limit).

• All tethers can be deployed from, or retrieved into, objects by means of user-definable scenarios. The deployment/retrieval dynamics model includes momentum effects of mass entering or leaving the domain of the tether itself, and produces related forces on objects deploying and retrieving the tether material.

• Tethers can be defined to have length dependent non-uniform material properties. Elastic cross section, aerodynamic cross section, and lineal mass density are independently specified for up to 15 separate regions. Properties at sub-nodal points within each region are determined by interpolation. Each region can have its own modulus of elasticity and material damping attributes.

• Tethers are subject to distributed external forces arising from the following environmental effects: aerodynamics in both the subsonic and upper atmospheric hypersonic orbital regimes; electrodynamics due to the interaction of current-flow with the Earth's magnetic field using current-flow models that incorporate the earth magnetic field and effects of an insulated or bare-wire conductor interacting with the orbital plasma environment model. Note, with an appropriate ribbon-to-plasma electron contact model, this could simulate grounding-current in a conducting elevator ribbon.

• Tethers can experience thermal expansion and contraction, gaining heat by direct solar radiation, earth albedo, earth infrared radiation, aerodynamics, and electrical currents; heat loss occurs through radiative dissipation.

• Tethers can be severed at multiple locations during simulation.

• Initialization can occur in many ways, including creating a stable configuration for extremely long tether chains, attached to and rotating with a planet (a space elevator) with due consideration for non-uniform tether properties and the concomitant longitudinally varying strain distribution of elastic tether material.

• GTOSS creates a database containing results of response to the user-defined material configuration, initialization specifications, and environmental options; this permanent data base can then be *post processed* to produce a wide variety of result displays, from tabular data, to graph plots, to animations.

3. Description of the Aerodynamics Model

Air loads on the space elevator are evaluated in the GTOSS subsonic aerodynamic regime. Air loads are calculated separately for each nodal segment, considering for each segment: its relative wind; its effective aerodynamic cross sectional area; and its atmospheric density. The tether's effective aerodynamic cross sectional area is a function of the position along the tether, specified independently of the elastic cross sectional area and mass density variations. The relative wind vector comprises contributions from both the wind disturbance and the tether's motion. Based, on this model, aerodynamic lineal-load-density is

determined from which total air load can be calculated on a nodal segment. Note that TOSS does not model a *twisting* degree of freedom (rotation about the *longitudinal* axis of the tether), thus, this model effectively presents the ribbon's full aerodynamic cross section to the relative wind at all times. If the relative wind changes in *azimuth*, then the tether will accordingly accommodate by assuming *a virtual twist* thus producing air loads corresponding to presentation of its maximum area to the wind; hence effects such as rotary flutter, twisting, and *differential windup* are not simulated.

This model is based on calculations often used to simulate kite aerodynamics, derived from a flat plate aerodynamics model. No aerodynamic interaction is assumed to take place between a ribbon segment and its adjacent segments, thus downwash precipitated by one segment does not induce effects on the adjacent segments. A raw *magnitude* of the total air load is found as the product of the dynamic pressure (derived from total relative wind) and the *effective projection* of the segment's surface area *normal* to the *direction* of the relative wind vector; this magnitude is multiplied by a flat-plate drag coefficient (typically between 1 and 1.5) to form the total air load. This resultant air load is assumed to act *normal* to the surface of the segment; segment orientation is derived from a tangent vector to the ribbon and the relative wind. Drag and lift are normal to one another (drag being aligned along the relative wind vector), with both lying in the plane defined by the relative wind vector and a tangent to the ribbon. Thus, the total air load vector is resolved into components *parallel* to and *normal* to the relative wind vector to calculate segment drag and lift densities for use in the GTOSS finite tether code.

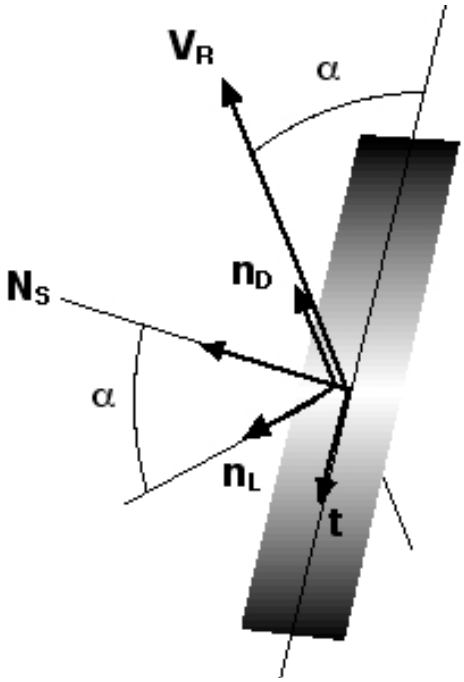

Figure 1 Ribbon Segment Diagram

Figure 1 above depicts an element of the ribbon acted upon by a relative

wind vector, $\mathbf{V}_R$. Below is an overview of the analytical relationships for this aerodynamic model.

$\mathbf{V}_R$ = relative wind vector acting at the ribbon element

$\mathbf{n}_D$ = unit vector in the direction of $\mathbf{V}_R$
(by definition = unit vector in the direction of Drag)

$\mathbf{n}_L$ = unit vector defining the direction of Lift
(by definition = unit vector normal to Drag)

α = angle between $\mathbf{V}_R$ ribbon tangent vector

$\mathbf{t}$ = unit vector tangent to the ribbon element

$\mathbf{N}s$ = unit vector normal to the ribbon element

A = area of the ribbon element

$\mathbf{A}$ = directed vector area of the ribbon element (= A $\mathbf{N}s$)

A_n = component of the element's area facing normal to $\mathbf{V}_R$

q = dynamic pressure

C_D = effective drag coefficient

F_A = magnitude of the total air load on the ribbon element

$\mathbf{F}_A$ = total air load vector on the ribbon element (= F_A $\mathbf{N}s$)

L = Lift on the ribbon element

D = Drag on the ribbon element

From these definitions and the geometry, it follows that,

$$\mathbf{N}s = \text{unit}[\, \mathbf{t} \times (\mathbf{n}_D \times \mathbf{t}) \,] \quad (1)$$

The component of area normal to the relative wind is,

$$A_n = \mathbf{A} \cdot \mathbf{n}_D \quad (2)$$

$$= A \sin \alpha \quad (3)$$

The total air load vector is,

$$\mathbf{F}_A = C_D A_n q \mathbf{N}s \quad (4)$$

Lift and Drag is then (in terms of "normal area component"),

$$L = \mathbf{F}_A \cdot \mathbf{n}_L = C_D A_n q \cos \alpha \quad (5)$$

$$D = \mathbf{F}_A \cdot \mathbf{n}_D = C_D A_n q \sin \alpha \quad (6)$$

Finally, Lift and Drag is,

$$L = C_D A q \sin \alpha \cos \alpha \quad (7)$$

$$D = C_D A q \sin^2 \alpha \quad (8)$$

This model, while not sophisticated, should provide a first approximation to the

aerodynamic loading on the space elevator. This model presents the tether's maximum aerodynamic area to the relative wind at all times; this can be thought of as differential weather-cocking along the ribbon's length to meet this assumption. This clearly disallows effects such as flutter; besides, such would require unsteady aerodynamics and torsional degrees-of-freedom for the tether, neither of which are included in the present TOSS model.

4. GTOSS Space Elevator Physical Properties

There are two elevator configurations used by GTOSS for studies; they will be referred to as the ***occupied*** and the ***unoccupied*** configurations. Both share the same *intrinsic* physical property description of the elevator ribbon. Within GTOSS, the unoccupied configuration logically constitutes a single tether and two objects, the objects being a ballast and a *pseudo object* (fixed to the planet serving as the anchor point). In the case of occupied configurations, an intermediate mass representing a climber is introduced on the ribbon; the occupied configuration is represented by two tethers and three objects, referred to in GTOSS parlance as a *tether chain* manifesting itself as a simple topological chain consisting of Object-*tether*-Object-*tether*-Object. By using appropriate definitions of tether properties above and below the *interior* object, the ribbon properties reflect that of the elevator's tapered design profile along the entire ribbon length.

A variation of the occupied configuration is used within GTOSS for purposes besides representing a climber. Since each finite tether model can have independent properties, assigning a different number of nodes to each tether can achieve dissimilar nodal resolutions at different regions of ribbon. For instance, in the case of aerodynamic studies, the nodal spacing required to provide proper resolution of wind profiles extending over the first 20 km, if used over the entire 100,000 km length of ribbon, would result in an impractical number of nodes. In this use, the *interior* object becomes a transition element within the chain, being assigned a mass commensurate with the nodal masses of the two adjacent tethers. It should be pointed out that tether frequency response characteristics is dependent upon its natural frequencies, and is proportional to its number of degrees of freedom, that in turn depends upon the node count. So the interface between two such tethers has the potential to be a band-pass filter, affecting transmission of disturbances. The power spectrum of response to disturbances can be examined, and if they are within the frequency response of both tethers, this should present no problem.

Unoccupied Elevator Configuration

Data characterizing the elevator configuration varies with length and comprises: mass density, elastic area and modulus, aerodynamic area, and damping properties corresponding to a preliminary baseline ribbon design described in References 1 and 2. A ballast mass of 634,000 kg, at a nominal radius of 100,000 km, produces 200,000 N tension at the ground. The elevator's dual tapered ribbon is nominally initialized by GTOSS to a stable vertical state with a ribbon longitudinal strain distribution that was in equilibrium with gravity

and centrifugal loading. The dual tapered ribbon is designed for optimally efficient material usage by achieving a uniform stress distribution over its entire length at a level of approximately half of the ultimate stress capability of 120 giga Pascal anticipated for an operational ribbon. GTOSS confirms this design objective as shown by the stress profile produced by the simulation, shown in figure 2.

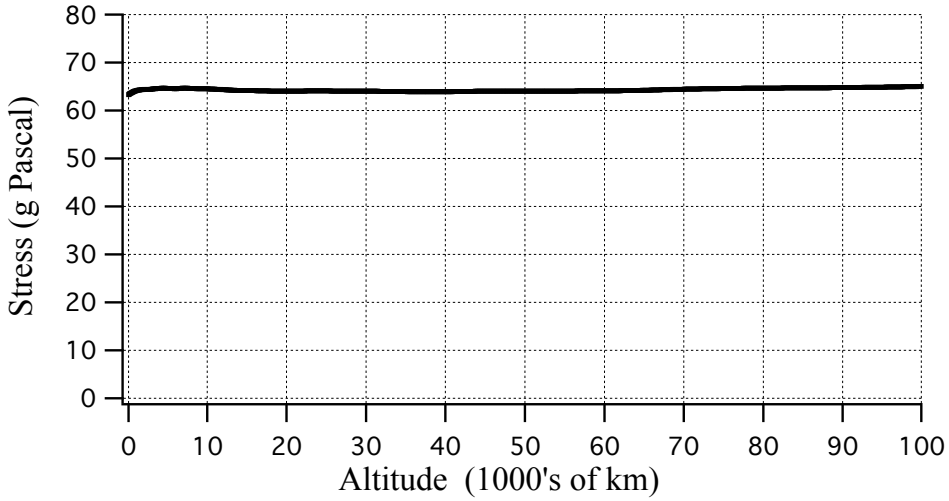

Figure 2. Ribbon Stress vs Altitude

This uniform stress results from the interplay of the ribbon's design profile for density, exponentially tapered elastic cross sectional area, and modulus that was used within GTOSS; these are shown in figures 3 and 4 below. The slight droop in the stress curve near the earth can be attributed to approximation errors associated with curve-fitting the ribbon profile's taper gradient near the earth.

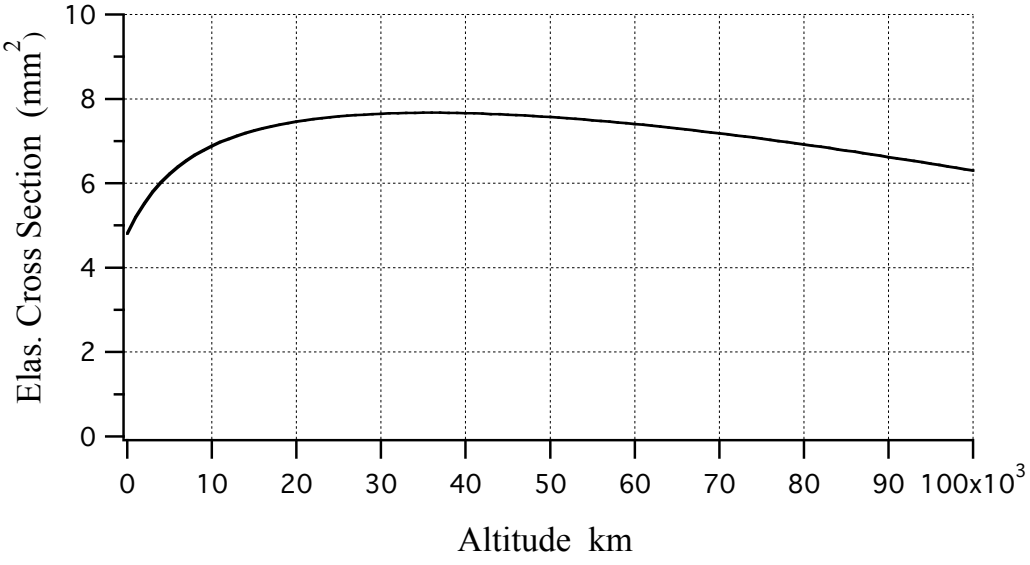

Figure 3. Ribbon Elastic Area vs Altitude

Based on the elastic cross sectional area profile and a nominal value of ribbon

material's bulk density of 1.3 gm/cm^3, the lineal density profile shown in figure 4 below was derived for use in GTOSS.

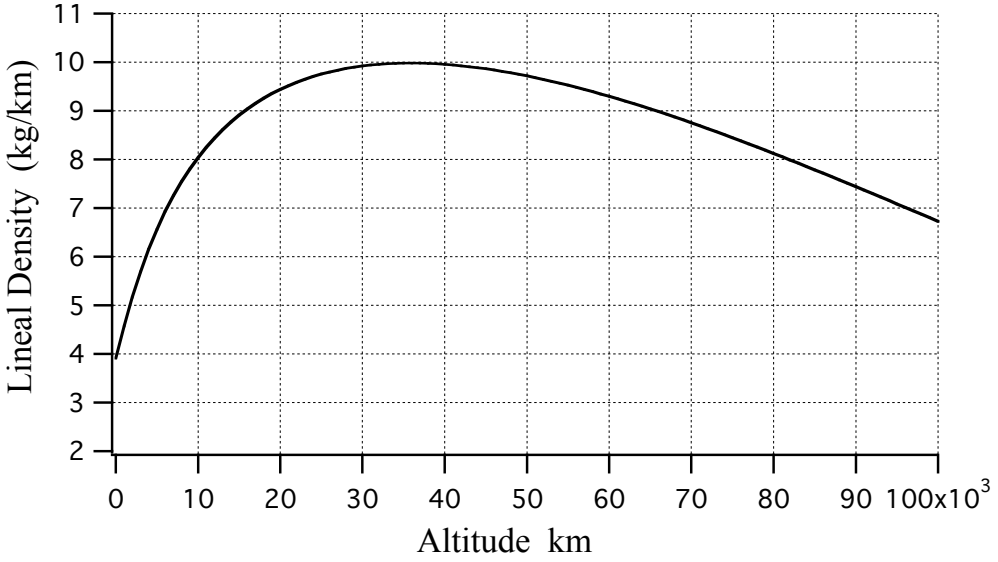

Figure 4. Ribbon Density vs Altitude

Occupied Elevator Configuration

The occupied elevator configuration requires the definition of two ribbon profiles, one ribbon deployed down to the earth, the other up to the ballast mass. GTOSS allows ribbon attributes to be assigned independently, so the *interior* object becomes the source object, from which two ribbons are *deployed* in opposite directions. One tether's deployed profile can be thought of as complementary to the other; thus, the end that would have emerged first downward corresponds to the earth end, while, that first deployed upward corresponds to attributes at the ballast end. Only for occupied elevators in which a climber is in transit would these tethers actually be undergoing time-dependent deployment. For static situations, the deployed ribbon length is automatically determined at initialization to produce a stable configuration. For all cases, except Case 2, the ribbon is assumed to have an *effective* aerodynamic width of 5 cm; this is referred to as an *effective* width to point out that it can be related to the actual ribbon width so as to factor-in design attributes such as wind permeability.

Occupied configurations are used exclusively in this study to allow both dissimilar nodal resolutions and enable the study of effects of climber presence on ribbon aerodynamic response. The climber has been assigned a mass corresponding to the nominal 20 ton design; an area of 18 m^2 is assumed in assessing the effects of drag on a climber. Due to its unknown attributes and preliminary design status, the climber has been simulated with three, rather than a six, degrees of freedom for this study.

Finite Element Resolutions

Dual levels of finite element spatial resolution (nodal spacing) were used throughout this study due to the impracticality of employing throughout the entire upper ribbon length the same resolution level required in the atmospheric regime. The spatial resolution in the atmosphere is about 300 times finer than that used for the ribbon above the atmosphere; the relative scale of this nodal resolution is depicted in various results plots. Either a climber mass was interposed between the two regions of nodal resolution, or, in the absence of a climber, a small mass on the order of a nodal mass was used. Results didn't appear to be sensitive to "interior object mass" selections within this nodal mass range.

5. Atmospheric Characterization

The area of the Pacific ocean, considered to be optimal for location for the space elevator, seems to have little quantified data for the wind environment at altitudes above sea level; thus it was concluded that at present, "probability of occurrence" type of synthesized wind-altitude envelops would likely not be meaningful.

Thus, for purposes of this study, a constant wind-versus-altitude profile was adopted as a reference. The wind level was allowed to buildup linearly with time, starting from no-wind and progressing to full-wind in a period of *two hours*. This was followed by a period of constant wind at peak level (typically two hours). Following this constant wind period, the wind level decreased linearly with time to zero over a period of two more hours. Figure 5 below, depicts this for the case of a Category 0 Typhoon, termed a "tropical disturbance". This study employed Category 0 (average of 25 m/s) and Category 3 (average of 54 m/s) wind levels.

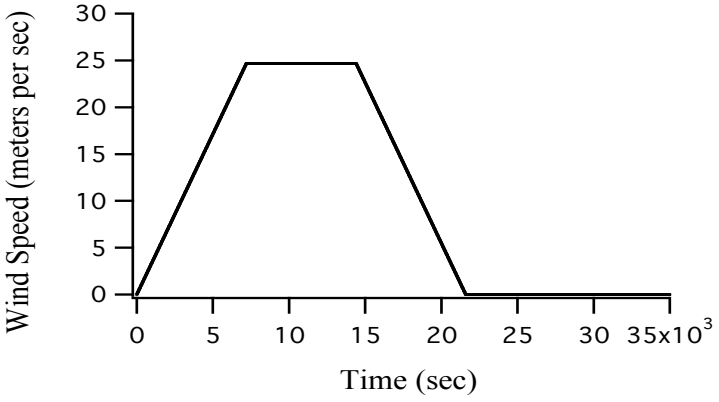

Figure 5. Wind Speed vs Time

Thus, most wind scenarios started with zero wind, and returned back to zero wind by 21,600 sec (about 6 hrs), with runs terminated after 10 hours (35,000 sec) of simulated time. For simplicity of results correlation, all winds blew from West to East, with no northerly component.

Important notes concerning plots:

- Many of the figures in this paper depict a series of *snapshots* of the data, taken at discrete times (frequently a series of more or less uniform time intervals of about 2000 sec).
- For snapshots taken during the initial 2 hour *build up of wind*, data is depicted by the *thinnest solid lines*.
- For snapshots taken during the duration of *peak wind* (2 or 4 hours), data is depicted by *thicker solid lines*.
- For snapshots taken during the 2 hour duration of *diminishing wind*, data is depicted with *long dashes*.
- For snapshots taken after the wind has *diminished again to zero*, data is depicted with *finer dashes*.

6. Case Definitions and Simulation Results:

Case 1: Unoccupied Elevator, Category 0 wind.

Case 2: ***Same as Case 1***, except ribbon width doubled to 10 cm.

Case 3: ***Same as Case 1***, except Category 3 wind.

Case 4: Climber parked at LEO at 200 nm , Category 0 wind.

Case 5: ***Same as Case 4***, except *peak wind* lasts 2 hours longer.

Case 6: Climber parked in Atmosphere at 9 km, Category 0 wind.

Case 1: Unoccupied Elevator Category 0 wind (Tropical Disturbance, 55 mph)

Figure 6 below consists of snapshots of the entire length of the ribbon, taken at approximately 2,000 sec intervals for 10 hours of simulated time. The Horizontal axis is *greatly exaggerated;* if these were depicted with identical vertical and horizontal scaling, this graph would appear as a single vertical line. Note, one ribbon snapshot is depicted by very fine dots, *each dot actually being a node* in the finite element model of the ribbon. This illustrates the level of spatial resolution of the GTOSS solution in this region, and is typical of all cases in this study. These snapshots clearly illustrate propagation of the disturbances caused by wind near the ground. When viewed from this grand scale, it is evident that perturbations due to wind are effectively equivalent to the response of a string subject to a transient boundary condition. The ballast mass, not depicted, terminates each ribbon snapshot at the upper end.

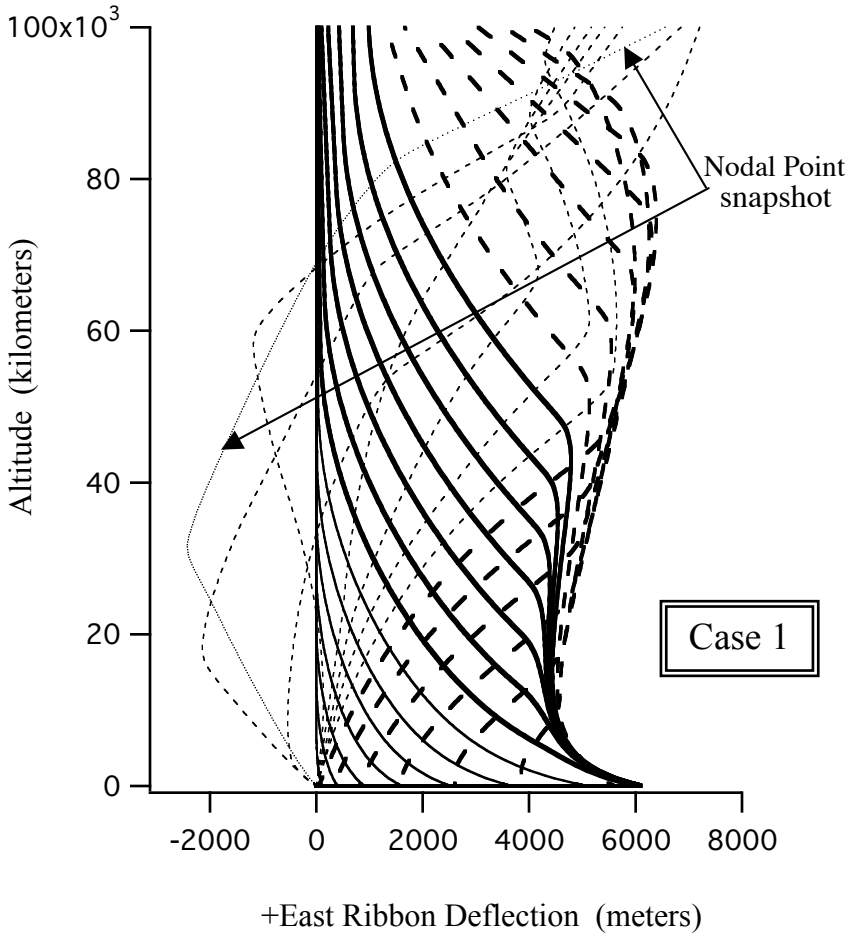

Figure 6. Snapshots of Horizontal Displacement vs Altitude

Examining figure 6 reveals that as the ribbon returns to vertical in response to recession of the wind, it overshoots, progressing westward. Upon arriving at the ballast mass, the ribbon's wind-induced horizontal displacement waves are seen to reflect off of the ballast mass for the return trip downward. The ballast mass is observed to start moving eastward as the ribbon's tension vector presents an east component at the ballast; it also appears that the ballast is about to undergo an overshoot to the east in response to this.

Figure 7 below, shows the near-earth ribbon snapshots of figure 6 above, except magnified and with identical vertical and horizontal scaling in order to depict true ribbon *departure angles* from the vertical. The one ribbon profile that is shown as ***dots***, depicts the nodes of the discrete ribbon model in the lower atmosphere; the level of resolution shown here is about 300 times finer than that in figure 6 above and extends up to 370 km.

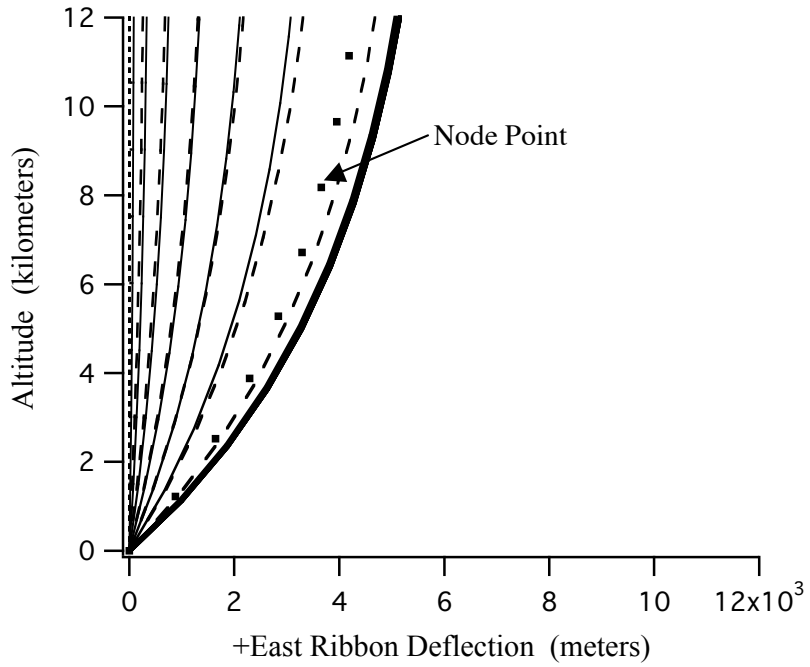

Figure 7. True-scaled Snapshots of Displacement vs Altitude

Examination of figure 7, (applying earlier stated conventions for snapshot-time representation), reveals that the ribbon progressively moves horizontally as the wind increases, then, holds position during the peak wind period as indicated by the overlapping of solid-line snapshots as seen on the far right side of the results envelope. The ribbon then returns to vertical as the wind subsides.

Figure 8 below presents an intermediate snapshot scaling.

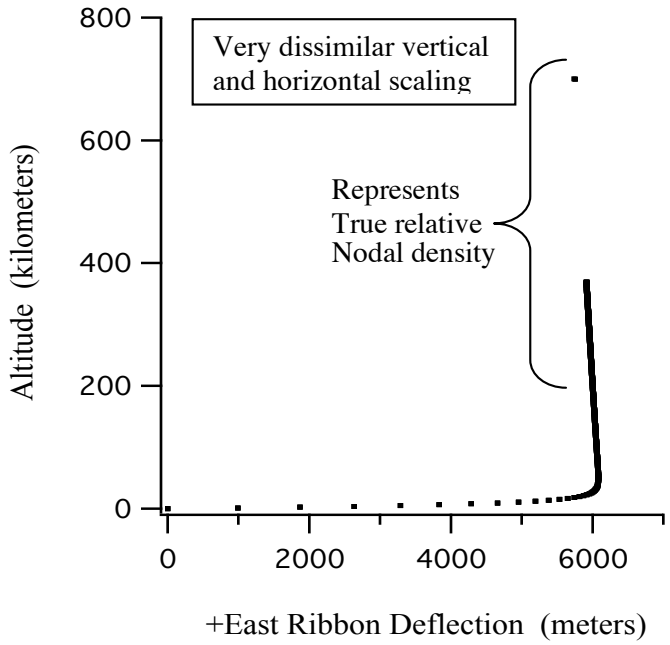

Figure 8. Intermediate-scale Snapshot of Displacement vs Altitude

The figure above shows the *relative spatial resolution* between the atmospheric region and that above by using dots at each nodal point. The single dot aligned above the solid segment is the first node encountered above the much higher nodal resolution within the atmosphere. Note that the figure's vertical and horizontal scaling is *significantly* different, thus making nodal spacing appear non-uniform where the ribbon curves to the horizontal; the apparent solid vertical line is representative of the atmospheric nodal-density as compared to that above shown by the single node (dot) whose position is consistent with the vertical scaling of the vertical line that appears to be solid.

Snapshots of air load *density* along the ribbon are shown in Figures 9 and 10 below. This is the total air load experienced per nodal segment (distance between

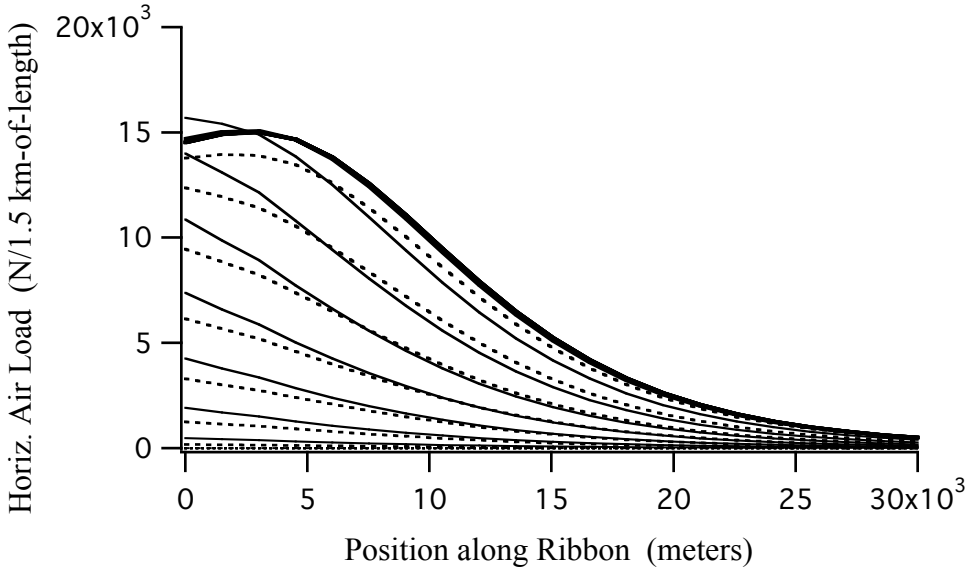

Figure 9. +East Comp. of Air Load Dens. vs Ribbon Arc Length

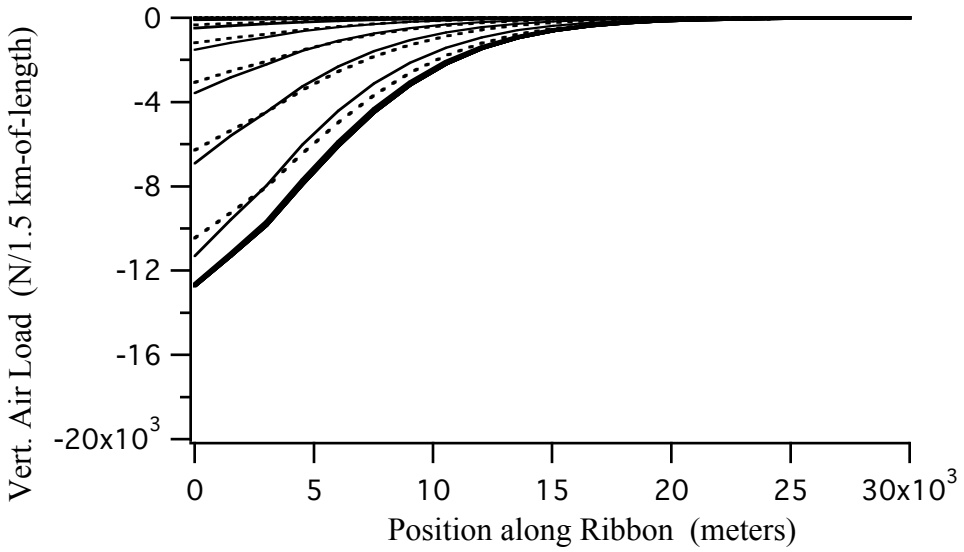

Figure 10. +Vert. Comp. of Air Load Dens. vs Ribbon Arc Length

nodes) versus arc length along the tether, which for Case 1 is essentially the altitude. Notice that there is a downward component of air load, a fact that is significant in later cases. With uniform wind, if the ribbon is vertical, then the air load profile reflects the atmospheric density-altitude profile. As the ribbon deflects significantly, geometrical considerations of relative wind and pressure calculations start to manifest themselves.

A stress versus ribbon-length snapshot envelope is shown in figure 11 below. Comparing this to the nominal unloaded stress profile shown in figure 2, shows there is little stress increase due to air loads which is consistent with the tension profile snapshot envelope shown in figure 12 below. The perturbation in stress near the ground is an artifact of interpolation of the ribbon's elastic property variation across dissimilar nodal spacing occurring at 370 km.

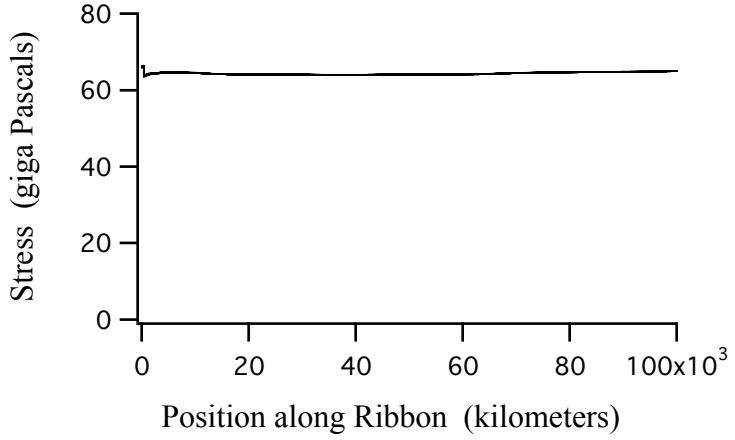

Figure 11. Stress Profile Envelope vs Ribbon Arc Length

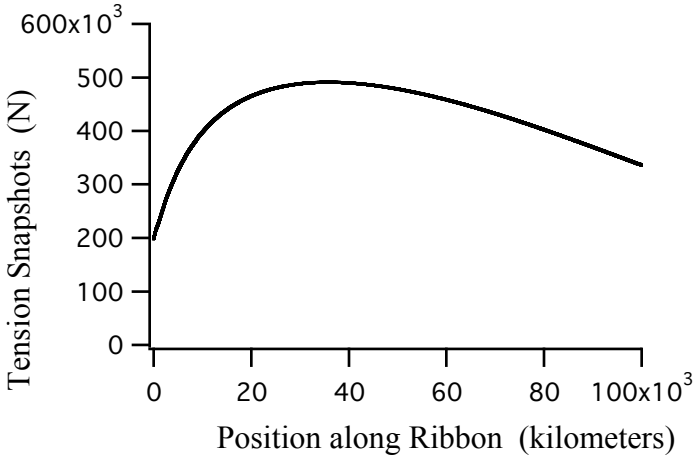

Figure 12. Tension Profile Envelope vs Ribbon Arc Length

Case 2: Same as Case 1, Except, <u>Ribbon Width = 10 cm</u>
Category 0 wind (Tropical Disturbance, 55 mph)

A narrow ribbon is desirable from a wind loading standpoint, but is likely not optimal for climber traction; the realities of design may dictate a wider ribbon.

Case 2 explores the effects of doubling the effective width from 5 cm to 10 cm.

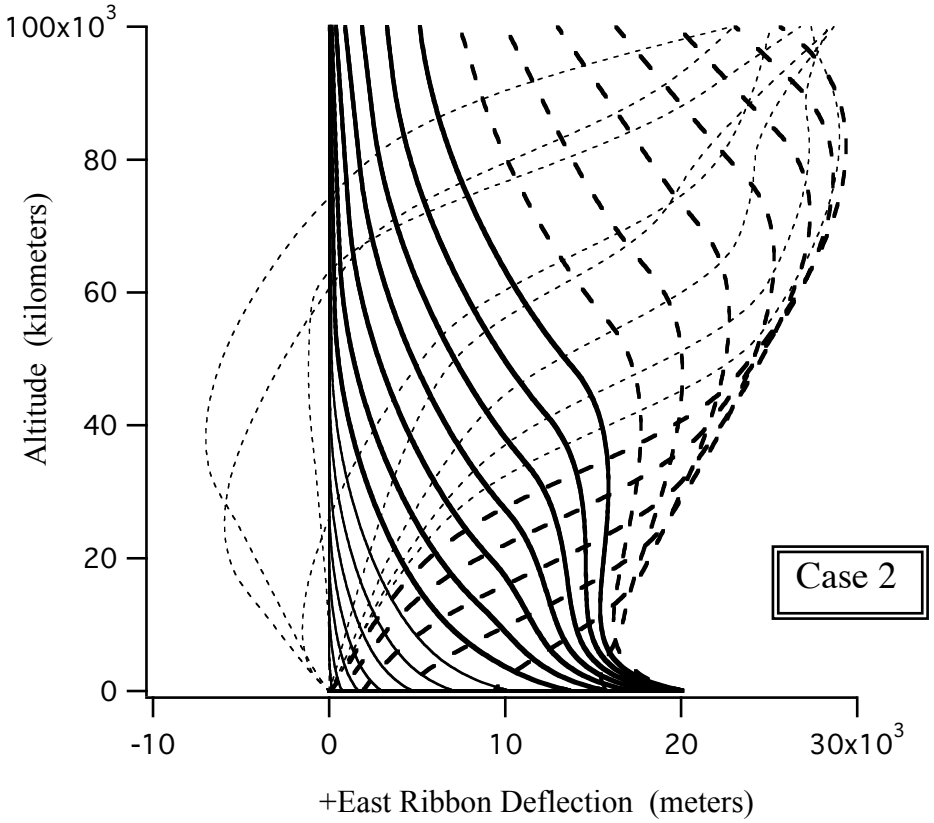

Figure 16. Snapshots of Horizontal Displacement vs Altitude

Figure 17 below shows a true geometrical depiction of near-ground response.

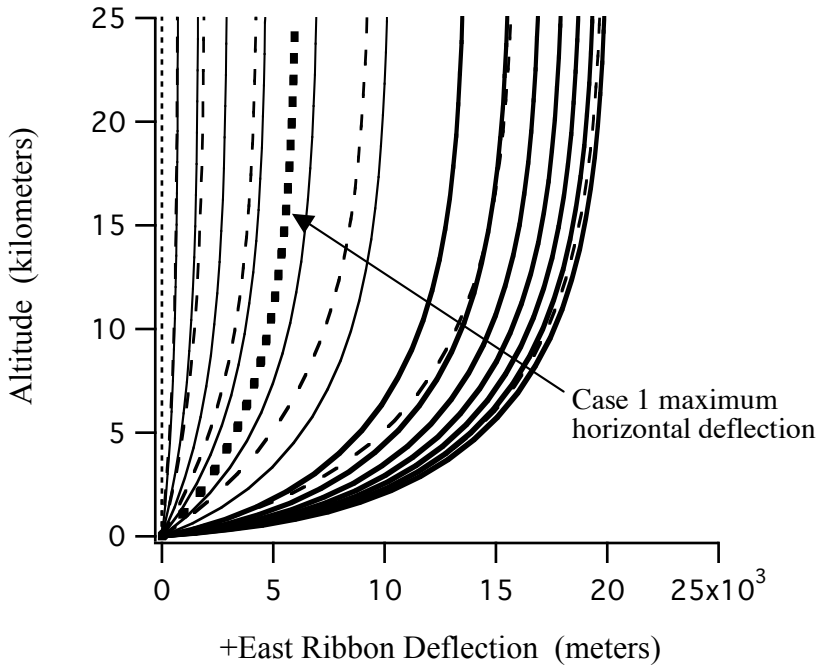

Figure 17. True-scaled Snapshots of Displacement vs Altitude

Significantly more horizontal displacement is seen than in Case 1. Doubling of ribbon width results in more than a tripling of horizontal displacement. Superimposed on this plot, as the heavy dashed line, is the maximum displacement from Case 1. This is an indication of a mechanism that may be inherent in the space elevator. Insight into this mechanism is gained by examining the air load distribution on the ribbon, shown in figures 18 and 19 below.

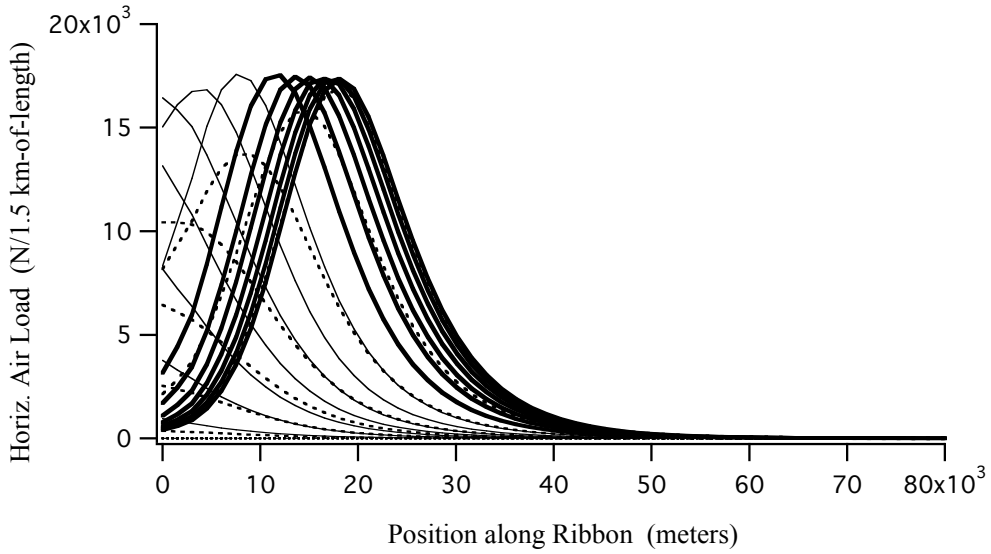

Figure 18. +East Comp. of Air Load Dens. vs Ribbon Arc Length

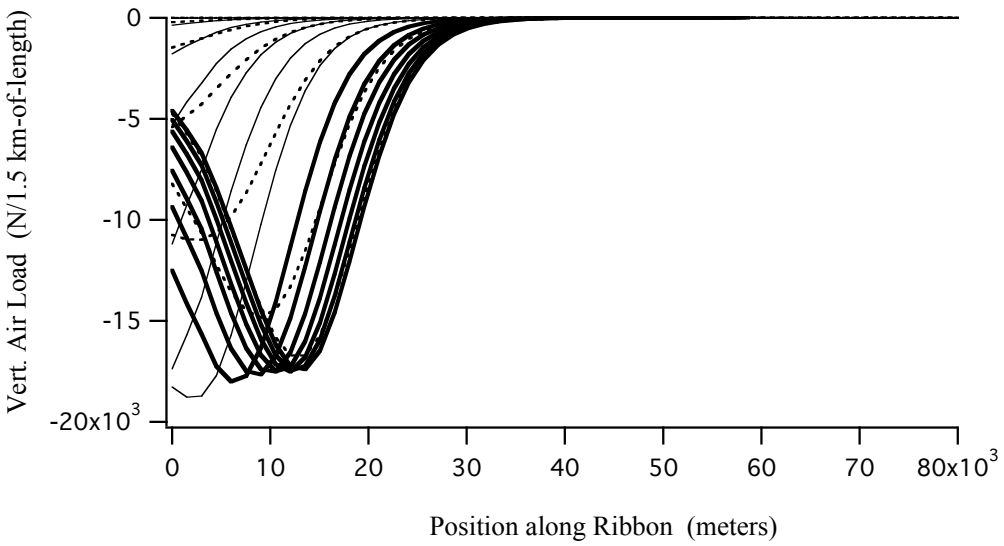

Figure 19. +Vertical Comp. of Air Load Dens. vs Ribbon Arc Length

These air loads, plotted against ribbon arc-length, are consistent with the ribbon's becoming increasing horizontal as seen by the migration of peak air load along the ribbon length. It is significant that the vertical-to-horizontal air load

ratios as well as *magnitudes* are migrating along the ribbon almost unchanged. Since there is no significant tension increase associated with this horizontal action, as seen in figure 20 below, it appears that there is no mechanism to

Figure 20. Tension-Snapshots Envelope vs Ribbon Arc Length

counter a tendency for the ribbon to be driven out horizontally, since the progressing horizontal displacement is resulting in little change to either the air load profile, or tension. Thus, once the air load intensity reaches a level for which its vertical and horizontal components can equilibrate the respective ribbon tension components, there may be little to counter further horizontal displacement. This supposition is indeed born out in the ensuing cases.

Case 3: Unoccupied Elevator
Category 3 wind (Tropical Typhoon, 120 mph)

Figure 21 below shows snapshots of the entire length of the ribbon, including the time of constant peak-wind and tail-off; comparing this to Case 1 (figure 6) indicates a factor of 100 greater horizontal response for the category 3 wind case than for category 0.

Figure 22 below shows magnified, near-earth, horizontal displacement snapshots with identical vertical and horizontal scaling to depict true geometry and ribbon *departure angles*; compare this to figure 7 (Case 1, Category 0 wind) to see the overall effects of wind speed on ribbon departure angle.

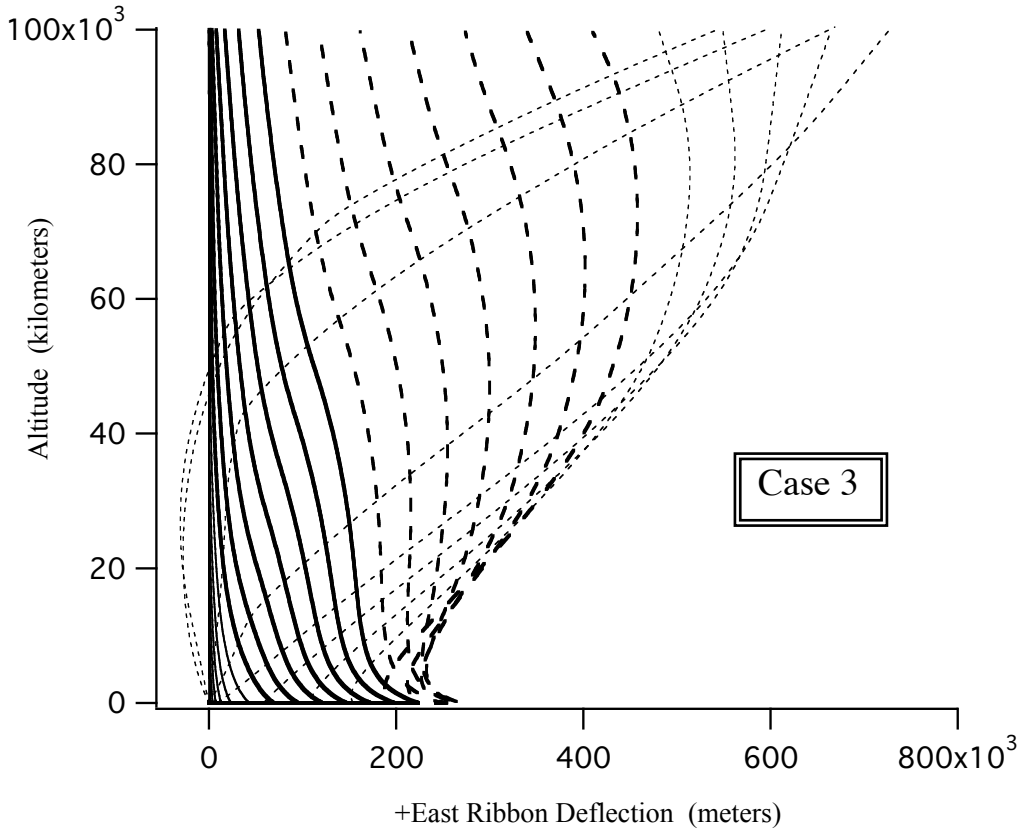

Figure 21. Snapshots of Horizontal Displacement vs Altitude

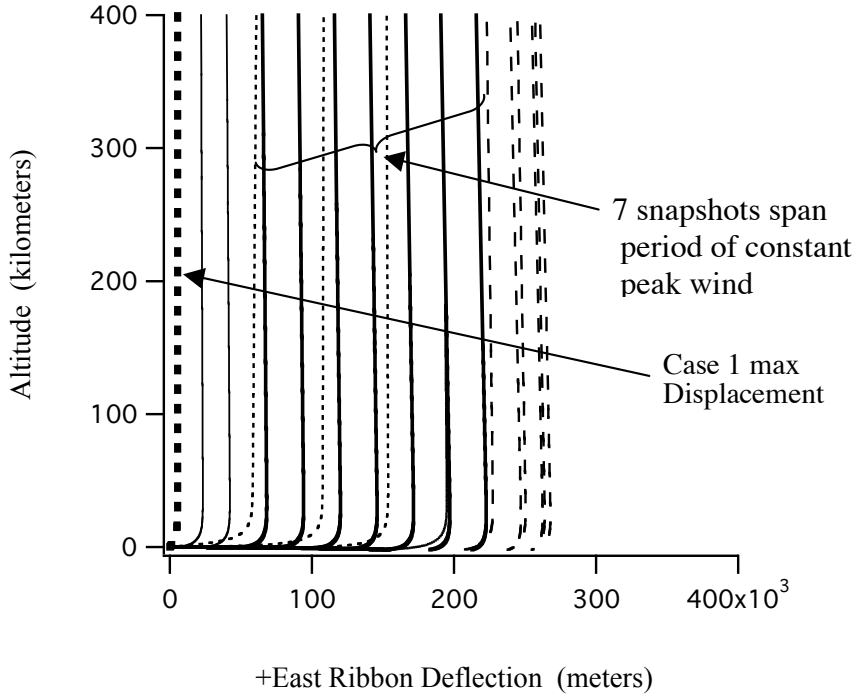

Figure 22. True-scaled Snapshots of Displacement vs Altitude

Note the single heavy vertical dashed line nearest the origin in figure 22 (above); this represents the maximum horizontal response of Case 1. It is evident that somewhere between category 0 and 3 wind levels, a threshold was reached for which wind force could overcome any inherent ribbon resistance to horizontal displacement. This supposition is further corroborated by the fact that the *bracketed* snapshots (with heaviest lines) near the middle deflections of figure 22, encompass exactly the period of constant peak wind, meaning that even with wind not increasing, the horizontal displacement continues to increase.

This case creates more stress response than Case 1, as shown in figure 23 below, but apparently this increase is incidental to the response rather than representing the advent of a significant horizontal restraining mechanism.

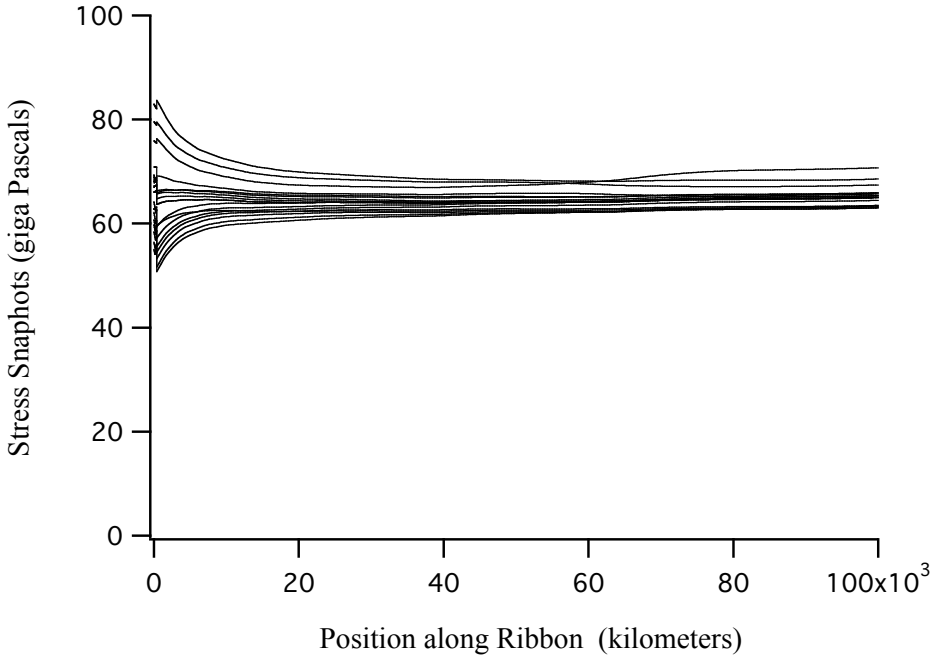

Figure 23. Stress Profiles vs Altitude

Case 2 and Case 3 expose the progressively increasing compliance of the ribbon to horizontal displacement in response to increasing wind load, regardless of whether the load is brought about by higher wind speed, or by greater aerodynamic width of the ribbon.

Case 4: Climber Parked on Elevator Ribbon at LEO (200 nm)
Category 0 wind (Tropical Disturbance, 55 mph)

Figure 24 below consists of snapshots of the entire length of the ribbon, taken at approximately 2,000 sec intervals for 10 hours of simulated time. Even subjected to identical winds, Case 4 exhibits vastly different response than Case 1 due to the presence of a 20 ton climber parked at 200 nm. Note the difference in

horizontal scale between Figure 24 and the equivalent plot for Case 1 (figure 6). Maximum horizontal ribbon displacement within the atmosphere for Case 1 was about 6,000 meters; for Case 4, the maximum displacement is 150,000 meters!

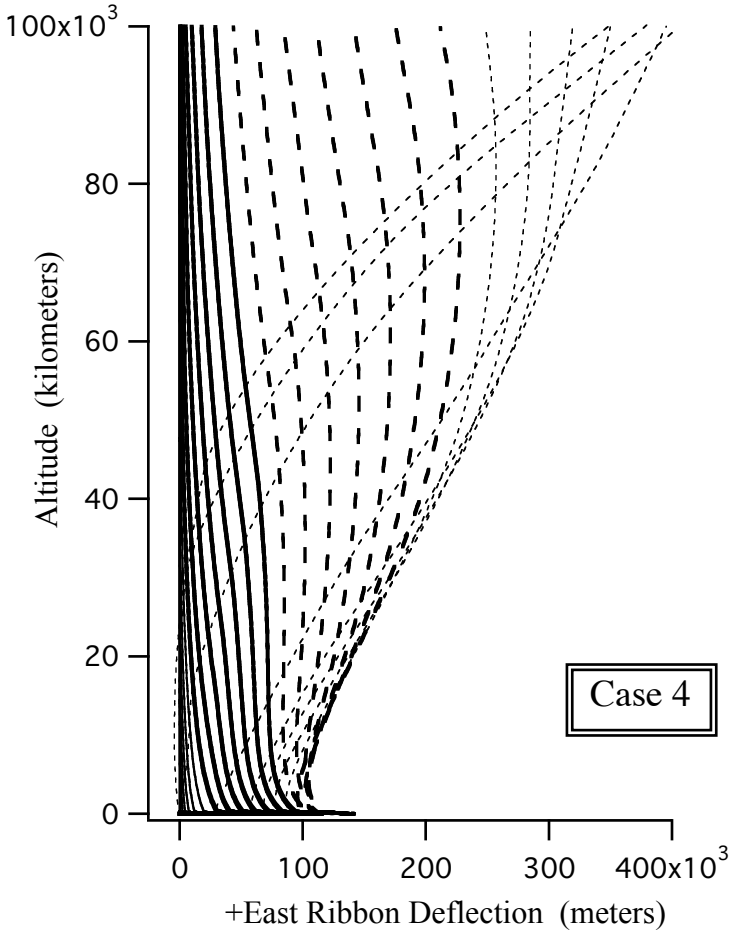

Figure 24. Snapshots of Horizontal Displacement vs Altitude

This can be attributed to the effect of climber mass that serves to modify response in the following two significant ways: (a) by presenting a significant inertia that affects ribbon excursions near the atmosphere, and (b) by creating a significant ribbon tension drop across itself (see figure 25), thus presenting to the atmosphere, a ribbon under 4 times less tension than in Case 1. The low tension presents a much more compliant ribbon to the wind than that of the unoccupied ribbon.

The tension discontinuity shown in figure 25 below occurs at the climber's position of 370 km altitude (200 nm).

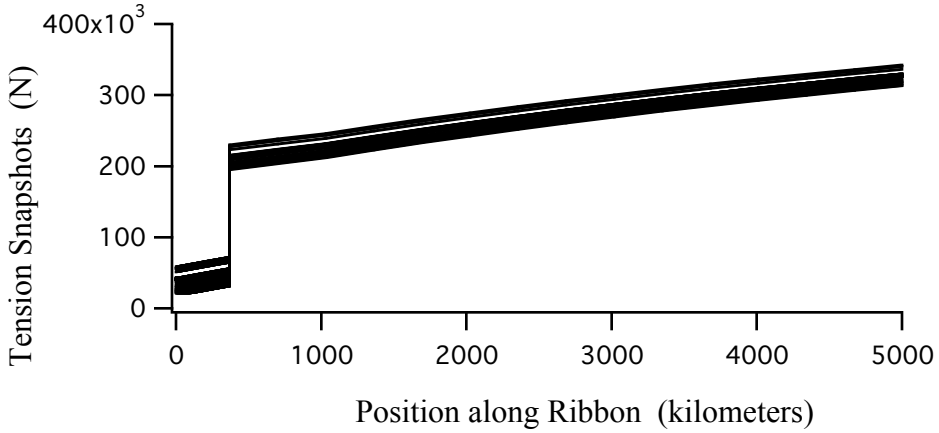

Figure 25. Snapshots of Tension vs Altitude

Snapshots in figure 26 below present identical scaling between the vertical and horizontal axes, thus depicting actual ribbon departure geometry, and indicates a ribbon eventually departing the anchor point at near horizontal. Note, that one of these snapshots is depicted with dots that represent the nodal resolution in this part of the ribbon.

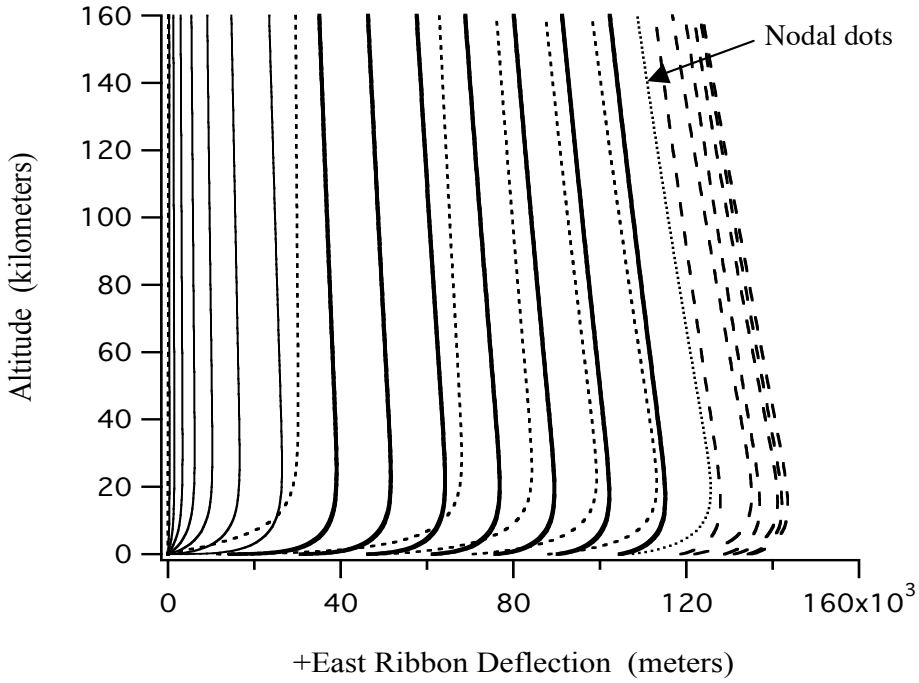

Figure 26. True-scaled Snapshots of Displacement vs Altitude

Figure 27 below is the same as figure 26 above, except with a much greater vertical scale to show the climber's position. Here, the sharp bend in the ribbon, not seen in figure 26 due to its scale, clearly depicts the location and effect of the climber. Note also the snapshot, composed of only dots at the nodal points; this shows where the nodal resolution changes at the location of the climber.

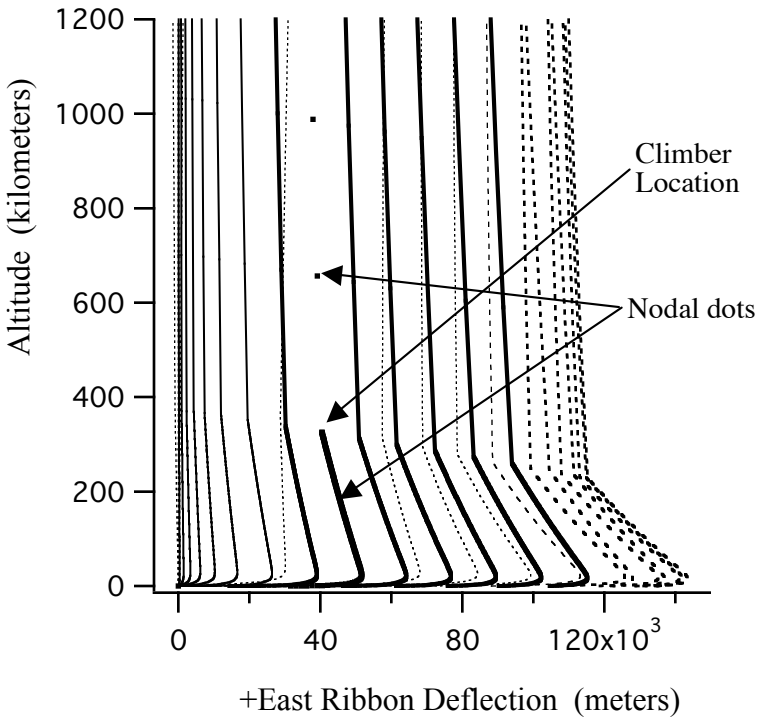

Figure 27. Snapshots of Horizontal Displacement vs Altitude

Figure 28 below has magnified but also *identically-scaled* vertical and horizontal axes to provide insight into the deflection mechanism in this case.

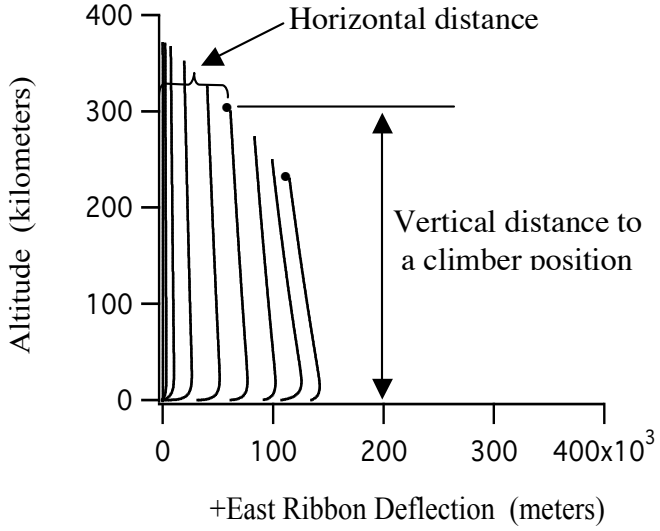

Figure 28. True-scaled Snapshots of Displacement vs Altitude

Figures 29 and 30 (below) show snapshots of air load versus *length* along the ribbon; these provide explanation of figure 28 above. Note that vertical air load is sufficient to equilibrate the vertical component of reduced lower ribbon tension between the climber and ground; therein lay the potential for the air loads to pull

the climber down. As the climber progresses downward, horizontal air load lays out the ribbon horizontally. Note, for each snapshot, the *sum* of the "vertical distance to the climber" plus the "horizontal distance to the anchor" is essentially constant, and equal to the initial vertical altitude of the climber. By the time the simulation has terminated, the climber has been displaced downward by about 140 km, accompanied by no significant tension increases. This is consistent with both the insignificant increase in upper ribbon strain corresponding to this climber displacement, as well as the upper ribbon's low effective end-to-end spring rate. Using an upper ribbon spring rate of 0.04 N/m, this decrease in climber altitude corresponds to a tension increase of 5000 N (out of 200,000 N extant in the ribbon above the climber); the corresponding strain increase in the upper ribbon due to this displacement is only 0.14 percent.

It is clear that the observed phenomenon depends upon the ability of the aerodynamic model to create vertical air loads.

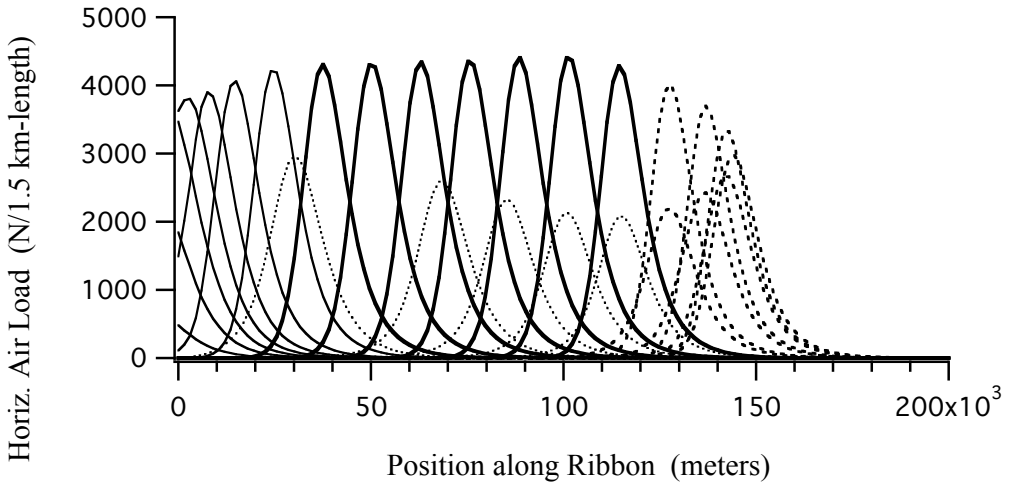

Figure 29. Snapshots of Horizontal Air Load vs Ribbon Arc Length

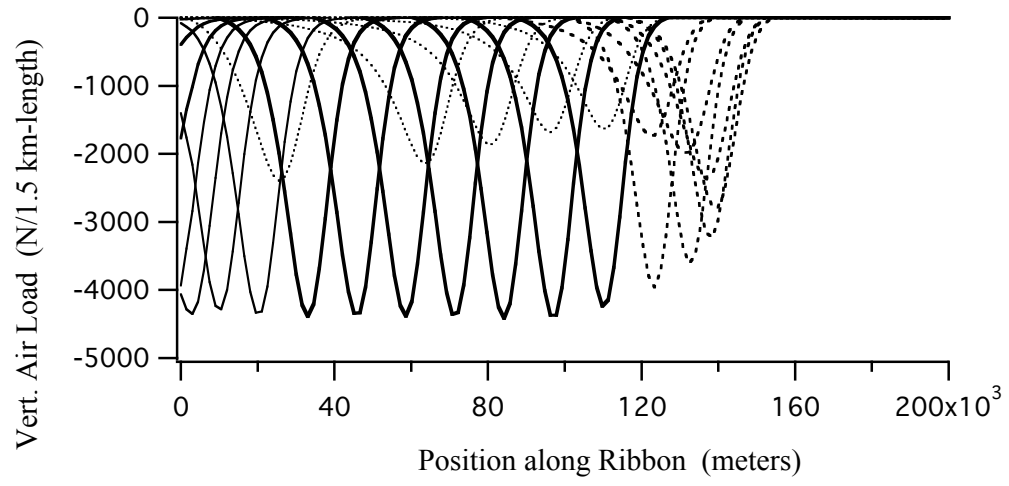

Figure 30. Snapshots of Vertical Air Load vs Ribbon Arc Length

Using the snapshot time-legend convention, the progression of air loads along the ribbon are again observed as in earlier cases. For example, the progression of air load along the arc length of the ribbon can be seen as the ribbon is laid down horizontally; this manifests itself by a snapshot's *traveling* along the ribbon. This is consistent with the aerodynamic model's predicting zero air load if the relative wind is parallel to the ribbon (as it would be if the ribbon were laying perfectly horizontal). Thus, regions of low (or no) air load are left behind as the load travels along the arc length of the ribbon. Note also that even after the wind has subsided, there are still air loads present; this is because the ribbon, in *springing back* to its vertical orientation, induces a relative wind on itself in the same direction and order of magnitude as that experienced under the original action of the atmospheric winds in producing the displacement.

It appears that once the wind-tension relationship reaches a point that the wind can lay the ribbon horizontal, then there may be insignificant natural restoring mechanism remaining. This progressive flattening phenomenon depends upon the air load being able to equilibrate both the horizontal and vertical components of ribbon tension beneath the climber. Since the ribbon bends from almost horizontal to almost vertical, and since tension is essentially constant over this region, this means that both the horizontal and vertical components of net air load must be nearly equivalent. Examining the displacement snapshots reveals an interesting feature at the point where the ribbon departs the horizontal and proceeds to vertical as shown in figure 31 below. The characteristic geometry of this transition region uniformly replicates itself from snapshot-to-snapshot, and presents a significant opportunity for vertical air load to be created by the aerodynamic model in GTOSS. This model describes a pressure distribution along the length of the ribbon, that creates a load vector normal to the ribbon's tangent at each point. Integrating this spatial force distribution around the curvature shown in figure 31 results in both a horizontal and vertical component of net air load. That a potential exists for similar magnitudes of net vertical and horizontal air loads is witnessed in figures 29 and 30 (above).

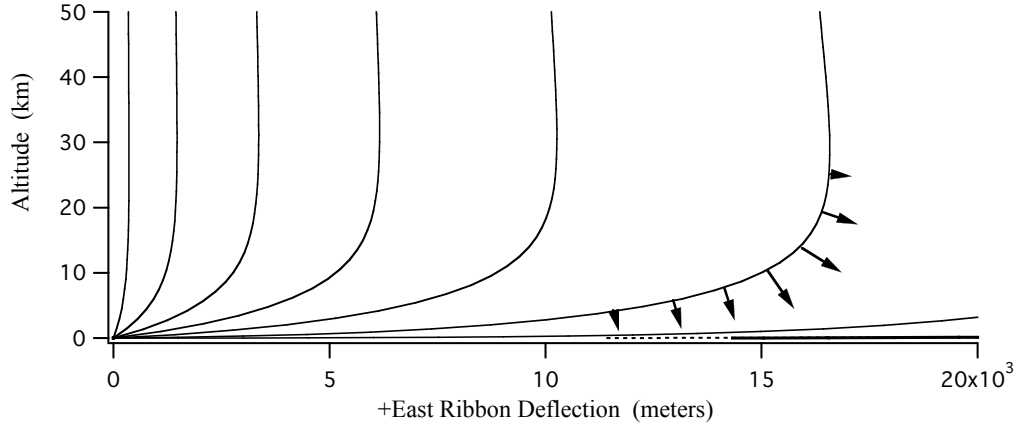

Figure 31. Snapshots of +East Displacement vs Altitude

Stress snapshots for this case are shown below in figures 32 and 33.

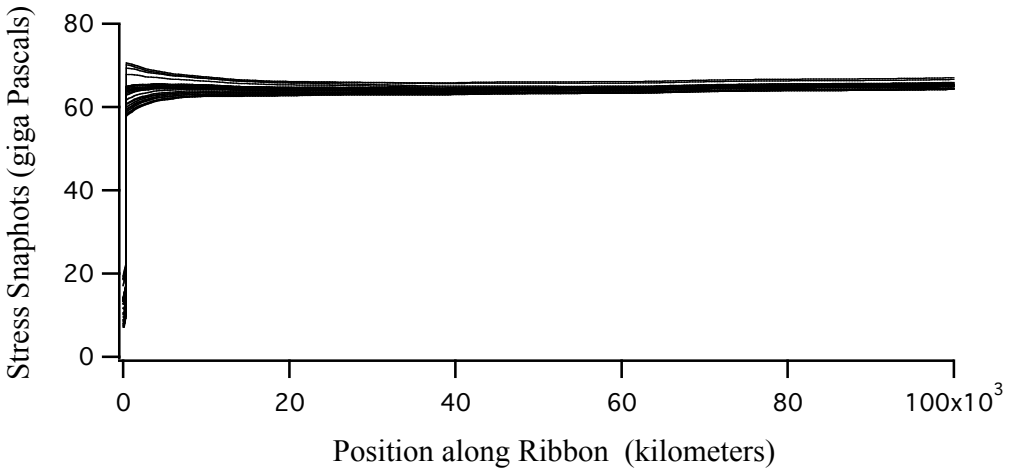

Figure 32. Snapshots of Stress vs Ribbon Arc Length

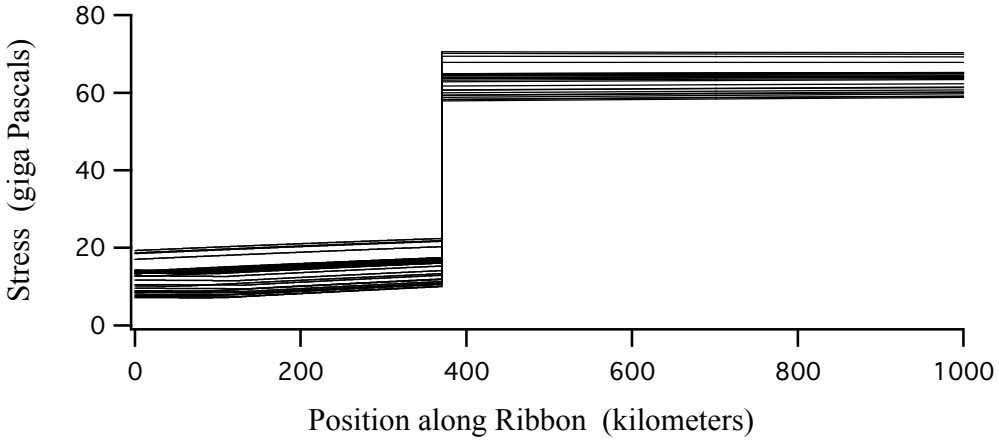

Figure 33. Snapshots of Stress vs Ribbon Arc Length

These indicate stress concentration near the climber, but are well below the factor of safety of 2. Stress drops significantly below the climber, positioned at 370 km on the ribbon, due to the low tension in this region of the ribbon.

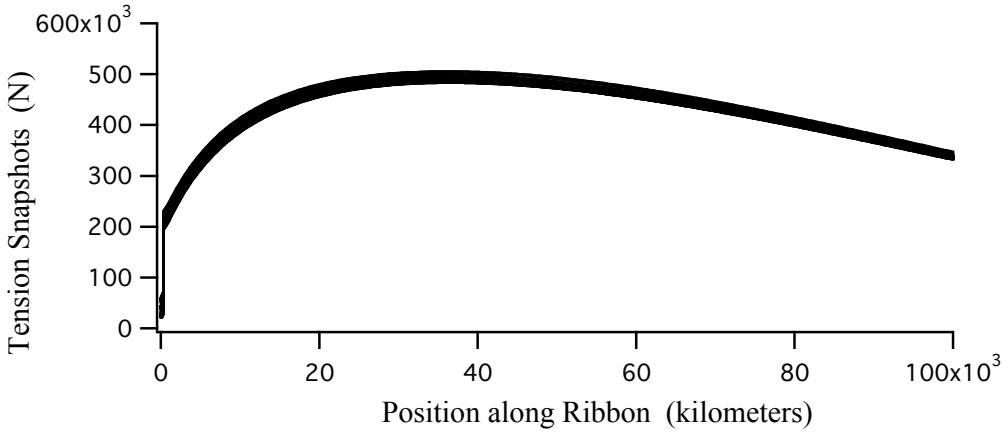

Figure 34. Snapshots of Tension vs Ribbon Arc Length

Case 5: Same as Case 4 above, Except: the Category 0 Peak Wind persists for 4 hours (rather than 2 hrs)

The results of Case 4 pose the question: once wind is sufficient to result in horizontal ribbon departure at the anchor, will there be natural mechanisms that will arrest this progression, or will the ribbon continue to be progressively displaced horizontally if the wind persists? This case explores this by allowing the peak wind of Case 4 to persist for 4 rather than 2 hours. Figure 35 below consists of snapshots of the entire length of the ribbon.

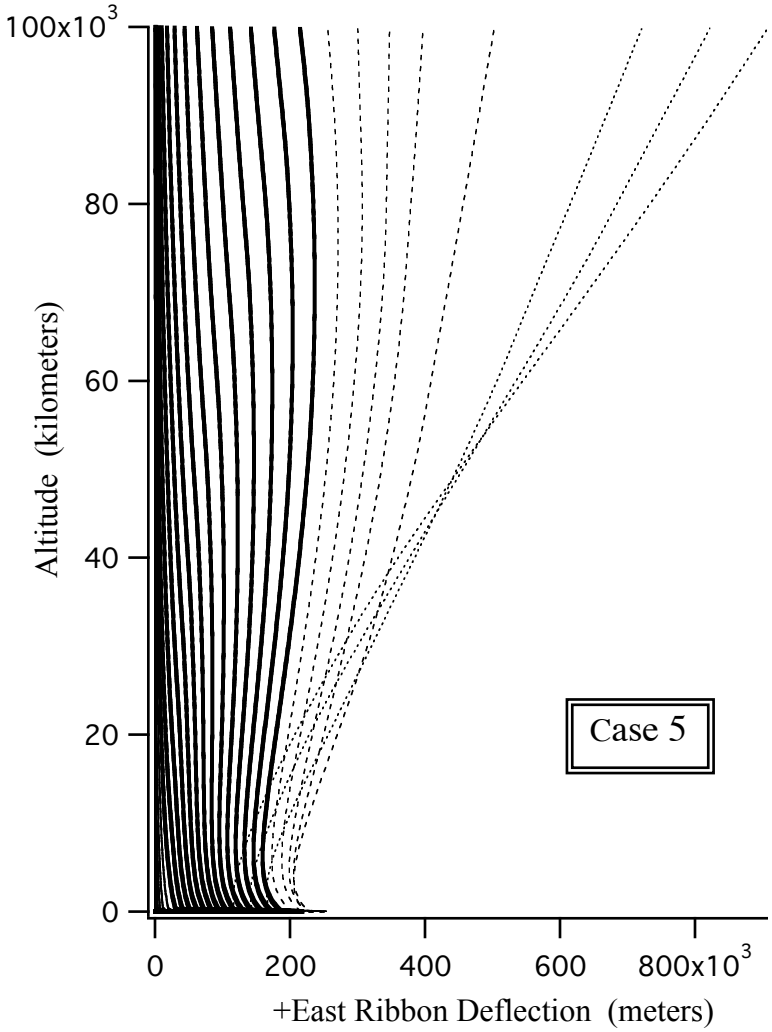

Figure 35. Snapshots of Horizontal Displacement vs Altitude

After 2 hours of peak wind, response in this case is identical to that of Case 4, however, of interest is what transpires thereafter during the additional 2 hours of peak wind. In figure 36 below, the maximum horizontal ribbon displacement for this Case 5 is compared to Case 4. It is seen that maximum displacements for Case 5 is nearly twice that of Case 4, correlating with the fact that Case 5 peak

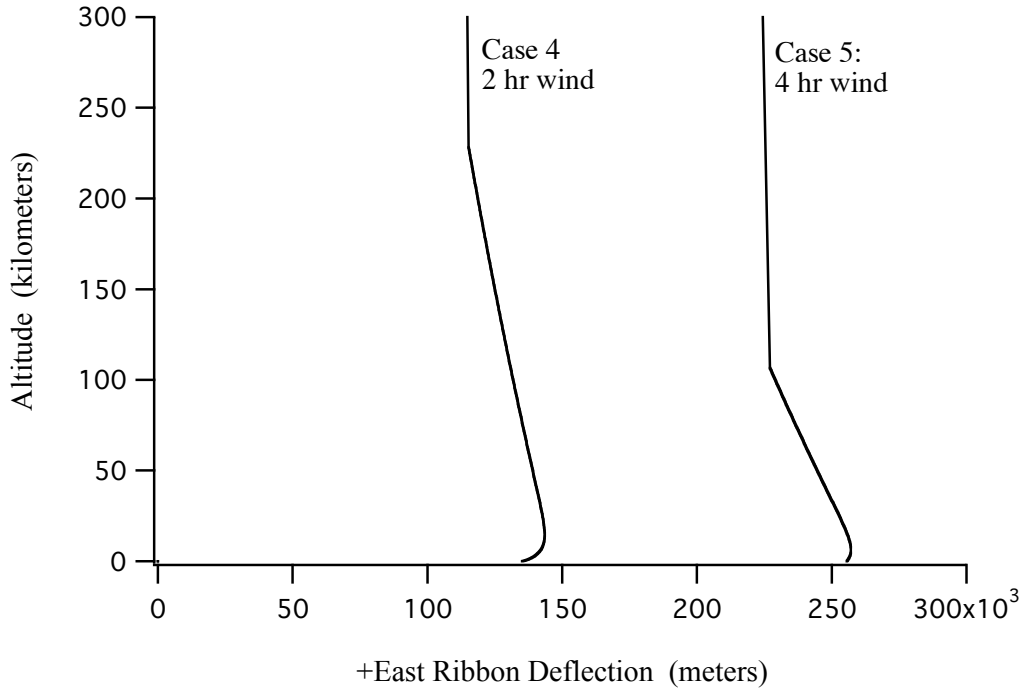

Figure 36. Maximum Horizontal Displacements vs Altitude

wind duration is twice that of Case 4. While this hints that the process may be self perpetuating, there also appears one or more mechanisms that may lead to natural arrest. Notice in figure 36 that as the climber (originally at 370 km altitude) gets drawn downward, the ribbon below it becomes increasingly *less* vertical. This functions to present a second component of horizontal ribbon tension countering the horizontal air load; however, concomitantly, the tension below the climber reduces slightly due to increasing gravity on the climber, countering the previous benefit. But more positively, as the horizontal displacement progresses, at some point, the geometry starts to resemble that of Case 6 below, that does have an inherent resisting mechanism.

Of all cases presented, this Case 5 exhibits the greatest ballast mass libration response. However, to put the extent of this in perspective, figure 37 below shows the libration of the ballast mass from its nominal vertical position, as viewed from the anchor point.

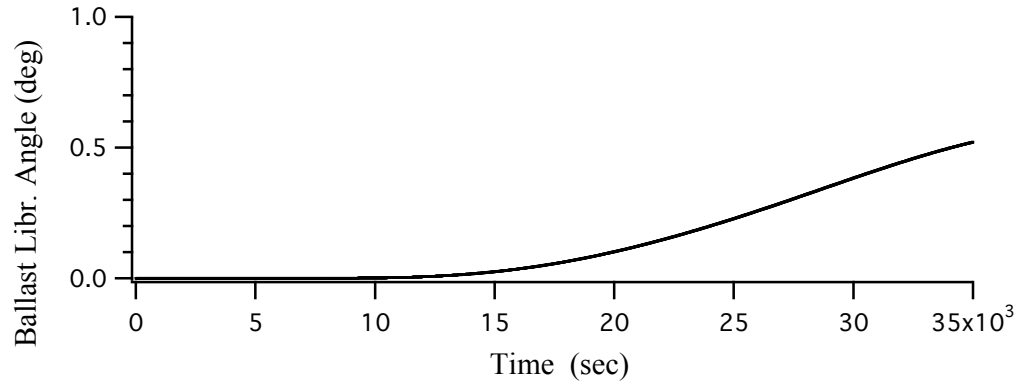

Figure 37. Ballast Mass Libration vs Time

It can be seen that even though the libration angle is still increasing at the termination of the run, it has reached inflection, and appears likely to peak well below 1 degree.

Case 6: Climber Parked on Elevator Ribbon at 9 km (30,000 ft)
Category 0 wind (Tropical Disturbance, 55 mph)

Here, a 20 ton climber is parked in the atmosphere at 9 km, and subjected to the Category 0 wind profile. Climber aerodynamics were characterized as a simple drag model with drag coefficient of 1.2 and cross sectional area of 18 m^2. Only horizontal air load is generated by the climber.

General response was typical of previous cases, so, only results of special interest are addressed here. Horizontal ribbon displacement is shown in figure 38 below. Note the one snapshot composed only of dots; this depicts nodal spacing below and above the climber, and shows a resolution below the climber that is *just adequate* to resolve aerodynamics; this sparseness was adopted for numerical efficiency. Location of the climber is evidenced by the sharp *bend* at about 9 km along the ribbon. This bend, while not pronounced near the ribbon's initial vertical position, ends up clearly depicted at a *horizontal* distance near 9 km; thus the trajectory of the climber becomes evident.

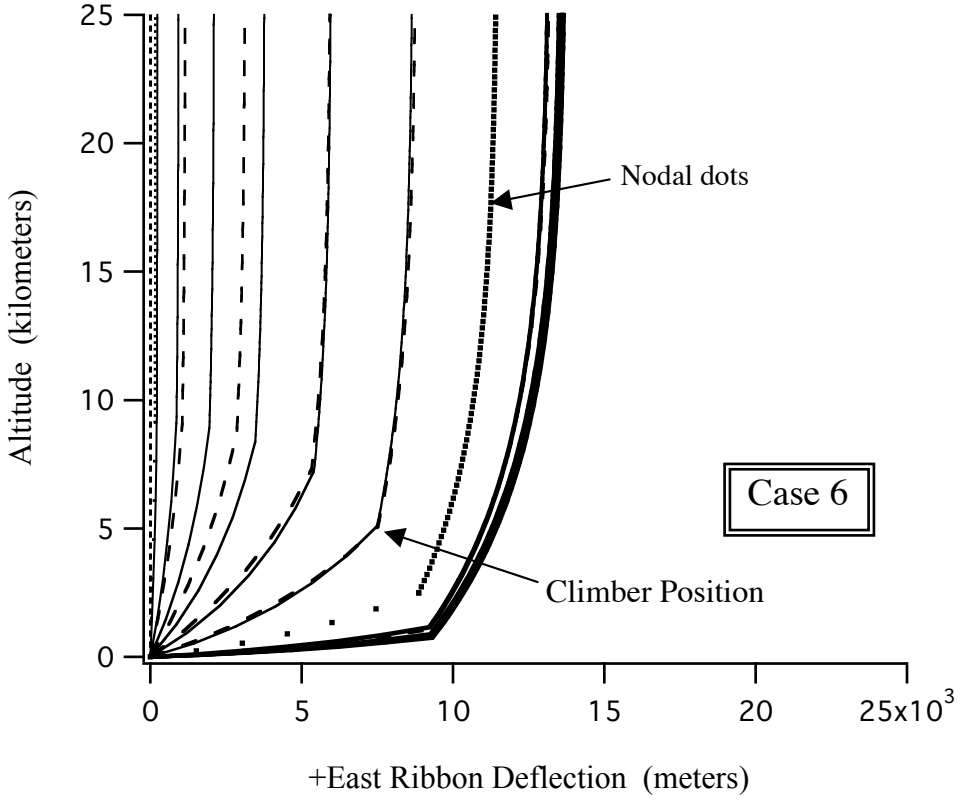

Figure 38. True-scaled Snapshots of Displacement vs Altitude

Due to the low tension between the ground and climber, there is little resistance initially to horizontal displacement of the climber; this is exacerbated even further by the additional atmospheric drag on the climber. So the climber and lower ribbon section easily move horizontally pulling the climber even lower; however, once the climber has moved a horizontal distance corresponding to its fixed position on the ribbon (of 9 km), then any additional action by air loads to move the climber horizontally is met by the now nearly horizontal segment of ribbon between the climber and ground. This short segment, with an effective spring rate about 10,000 times greater than the ribbon above, can easily equilibrate any horizontal load with very little additional strain as shown in figure 38 above. A tension time history in the lower ribbon segment is shown in figure 39 below. This shows that the tension rises to meet the applied horizontal air load, thus effectively constraining the climber from additional horizontal motion. Once the lower ribbon becomes near horizontal, the situation then mimics the displacement, shape and departure angles of the unoccupied elevator, as witnessed by the fact that in this Case 6 the ribbon above the climber exhibits about 5 km of maximum horizontal displacement *beyond the climber;* this compares closely with the shape and peak displacement of the unoccupied elevator (see figure 7). Comparing cases 1, 4 and 6, all subjected to identical winds, reveals that Case 6, yielding 14,000 m of maximum horizontal displacement, is closer to the unoccupied elevator Case 1 (6,000 m) than that of Case 4 with the climber parked at 200 nm (150,000 m).

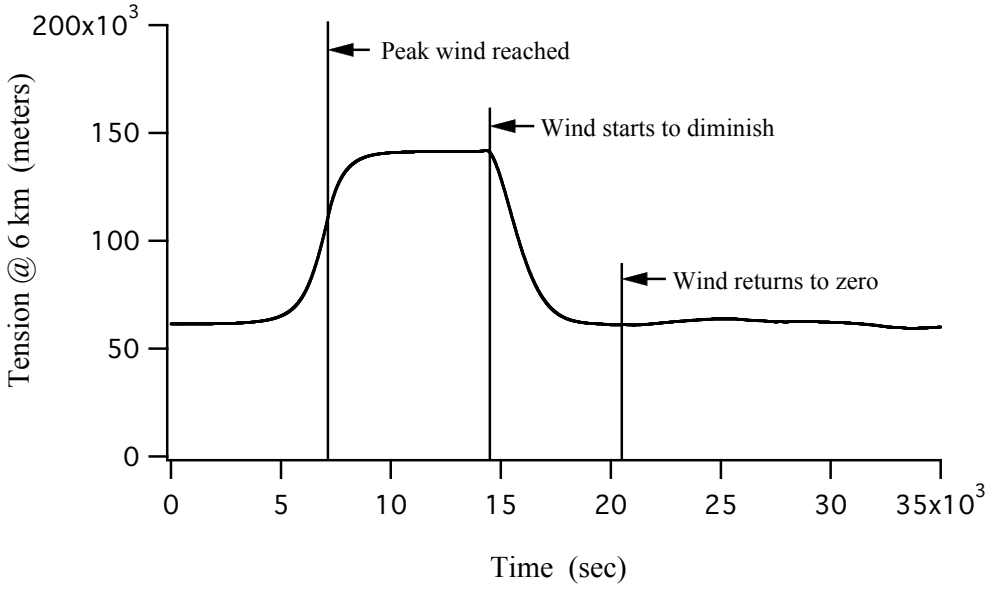

Figure 39. Tension between Ground and Climber vs Time

7. Discussion of Results

There were two general elevator behaviors exhibited in this study that bear specific discussion: One was the absence of over-stress to wind loading even with resultant large horizontal displacements; the other was the apparent ease with which the wind could drive the ribbon out horizontally.

The absence of over-stressing can be attributed to a combination of the following:

1. The overall ribbon has an extremely low effective end-to-end spring rate at earth on the order of .04 N/m. This mean that relative to local atmospheric disturbance, the ribbon can tolerate a significant amount of elongation without significant rise in tension.

2. A ribbon departure of even 200 km downrange, while appearing significant from an anchor-station viewpoint, and presenting a bizarre ribbon departure of near horizontal, in fact represents a minimal increase in overall strain of the 100,000 km long ribbon.

3. The fact that stress wave propagation time (approximately 1 hour to travel 100,000 km) is very short compared to the time it takes a strong wind to build up. This effectively defuses the possibility of localized stress at the source of the disturbance by quickly propagating stress gradients upward along the entire length of the ribbon, distributing strain.

Understanding the propensity for the wind to blow the ribbon horizontally downrange can be attributed to the aerodynamic model and the ribbon geometry as it yields to the relative wind. In order for the ribbon to sustain horizontal displacement, it is necessary for the vertical and horizontal components of air load to equilibrate respectively the vertical and horizontal components of ribbon tension. The aerodynamic source for this equilibration arises over a region of essentially uniform curvature as the ribbon departs the horizontal and proceeds upward to vertical.

The aerodynamics model used in this study predicts that if the relative wind has any component normal to the ribbon, then a pressure against the ribbon results, and a force normal to a tangent to the ribbon results. The vector integral of this force distribution provides the required horizontal and vertical force components.

8. Conclusions

While the wind profiles employed were simplistic and synthetic, likely representing the worst case profile (but not level), inherent response tendencies have been revealed. Assuming that the aerodynamic model is reasonably representative of nature, it appears that a strong wind can potentially create near horizontal ribbon departure angles at the anchor. The degree to which the elevator is susceptible to such response depends upon the presence and location of a

climber. Once the wind reaches a strength for which aerodynamic forces alone can equilibrate vertical ribbon tension, then new factors come into play. Under an extreme wind scenario, ballast is subject to being displaced downward weakening resistant to further additional horizontal ribbon displacement. Thus it appears that in such a scenario, the limiting factor may be the geographical and temporal bounds of the wind; for instance, is a storm large enough in size, or long enough in duration to threaten the elevator?

It appears that if the elevator is rendered dysfunctional due to wind loading, it will not be a result of over-stress, but rather due to ancillary considerations. To cope with potential horizontal departure angles, the ribbon anchor point may need to be mounted atop a tower or mast structure such as seen in offshore drilling rigs. It appears that a ribbon design criteria may require tolerance to ocean spray and salinity.

9. Future Work

This study made no attempt to quantify wind altitude-dependency or statistical properties, so it is not possible, based on these results alone to assess wind vulnerability of an elevator from an operational and statistical viewpoint; such an assessment would be a next step. This will require the acquisition of more definitive wind data for the proposed elevator locale. With such data, GTOSS can characterize resulting wind response to support Monte Carlo analyses, thus more realistically defining the impact of wind on real space elevator operations. Further quantification of the effects of wind duration should be explored, as well as response to gust environments.

Acknowledgements

Funding for this work has been provided by the Institute for Scientific Research, Fairmont, WA.

References

1. Edwards, Bradley C., Westling, Eric A. "The Space Elevator", published by Spageo Inc, San Francisco, CA, 2002.

2. Edwards, Bradley C., unpublished communications with the author.

3. Pearson, Jerome, "The Orbital Tower: a Spacecraft Launcher Using the Earth's Rotational Energy", Acta Astronautica. Vol. 2. pp. 785-799